ISSN 2618-1584 Vol. 6, Issue 12: 72-82, DOI: 10.25236/FMSR.2024.061211

# The mechanism of Ets1/Mgl-1 pathway impairment of circovirus B protein D

**Nuo Chen, Yu Han, Rongzhou Wu***

*The Second Affiliated Hospital of Wenzhou Medical University, Wenzhou, Zhejiang, 325027, China*
*wrz71@hotmail.com*
**Corresponding author*

***Abstract:*** *The aim of this study was to investigate the protective effect of Cyclovirobuxine D (CVB-D) in myocardial infarction model and its potential molecular mechanism. By establishing an animal model of myocardial infarction and a cell model induced by hypoxia in vitro, we observed that CVB-D can alleviate tissue damage after myocardial infarction, improve cardiac function, and reduce cardiac fibrosis. At the cellular level, CVB-D enhanced autophagy and patted autophagy flow in cardiomyocytes after hypoxia, which was manifested as an increase in the ratio of autophagy related protein LC3-II/I, an increase in Lamp1 expression and a decrease in p62 expression. Further molecular mechanism studies suggest that CVB-D may promote autophagy of cardiomyocytes by activating Ets1/Mcl-1 signaling pathway and alleviate myocardial cell damage caused by hypoxia. These findings provide new strategies and potential drug targets for the treatment of myocardial infarction, as well as new insights into the mechanism of autophagy regulation in cardiomyocytes under stress. Future studies will continue to explore the potential application of CVB-D in the treatment of cardiovascular disease and further elucidate its molecular mechanism of action.*

***Keywords:*** *Cyclovirobuxin D (CVB-D); Myocardial infarction; Ets1/Mgl-1 signaling pathway; Molecular mechanism; Myocardial cell autophagy*

## 1. Introduction

Myocardial Infarction (MI), a serious process of myocardial tissue ischemia and hypoxia resulting from blocked coronary blood flow, is the leading cause of death worldwide [1,2]. Although modern medicine has made remarkable progress in the treatment of myocardial infarction, the search for more effective treatment methods to reduce the mortality and improve the quality of life of patients with myocardial infarction is still the focus of medical research.

In recent years, Cyclovirobuxine D (CVB-D), as a natural compound, has been shown to have a protective effect on cardiomyocytes in several studies [3,4,5]. However, its specific protective mechanism in myocardial infarction models has not been fully elucidated. Autophagy, as a cleaning mechanism inside cells, can maintain the survival of cardiomyocytes after myocardial infarction by degrading damaged cell components [6-7]. Studies have shown that the activation of autophagy can help alleviate the damage and apoptosis of cardiomyocytes [8], but its regulatory mechanism is still not fully understood.

The purpose of this study was to explore the specific protective mechanism of boxyline in myocardial infarction model. In particular, it plays a role in hypoxia-induced autophagy of cardiomyocytes through Ets1 (E26 Transformation-Specific Sequence 1) transcription factor and Mcl-1 (Myeloid Cell Leukemia-1). Through in vivo and in vitro experiments, we expect to reveal that boxboxine can promote autophagy of cardiomyocytes, smooth autophagy flow, alleviate myocardial injury, and improve cardiac function by regulating Ets1/Mcl-1 signaling pathway.

In this study, the animal model of myocardial infarction and the cell model induced by hypoxia in vitro were established to simulate the environment of myocardial infarction. Subsequently, the effects of boxylline on myocardial tissue and cells were observed through drug intervention. Western Blot was used to detect the expression levels of Ets1 and Mcl-1 in myocardial tissue, while the changes of autophagy related protein expression and Ad-mCherry-GFP-LC3B dual fluorescence indicator system were used to detect the changes of autophagy flow. In addition, the protective effect of buxine on the heart after myocardial infarction was comprehensively evaluated by means of cardiac ultrasonography, TTC staining and Masson staining.

ISSN 2618-1584 Vol. 6, Issue 12: 72-82, DOI: 10.25236/FMSR.2024.061211

Through this study, we expect to provide new theoretical basis and potential drug targets for the treatment of myocardial infarction, and provide new insights into the mechanism of autophagy regulation of cardiomyocytes under stress conditions. This has important implications for developing new therapeutic strategies to improve the prognosis of patients with myocardial infarction.

## 2. Materials and methods

### *2.1 Establishment and grouping of animal models*

The C57BL/6 male mice used in this study were all purchased from Beijing Weitonglihua Experimental Animal Technology Co., LTD., and were strictly kept in a specific pathogen free (SPF) environment in the Experimental Animal Center of Wenzhou Medical University to ensure constant temperature and humidity conditions to maintain the best physiological state of the animals.

Model construction: C57BL/6 male mice aged 8 weeks were selected as experimental objects. Prior to model construction, mice were anesthetized by isoflurane inhalation, followed by tracheal intubation to maintain respiratory access, and permanent ligation of the left anterior descending coronary artery (LAD) was performed under a microscope to construct a myocardial infarction model.

Group and treatment: Fifty 8-week-old C57BL/6 male mice were randomly and evenly allocated to the following four experimental groups: ①Control group (normal control group) : The same amount of distilled water was injected intritoneally every day; ② CVB-D group (simple drug control group) : 1.0mg/kg CVB-D was intraperitoneally injected daily; ③MI group (myocardial infarction group) : the same amount of distilled water was injected intraperitoneally every day; ④MI+CVB-D group (molding administration group) : 1.0mg/kg CVB-D was intraperitoneally injected daily.

### *2.2 Establishment and grouping of cell models*

(1) Preparation and culture of primary cardiomyocytes: The primary cardiomyocytes were isolated and cultured from the heart tissue of C57BL/6 mice at 1-2 days of age through fine digestive treatment and differential adhesion techniques. The cells were randomly divided into three groups: Control group (normal control group with no treatment), Hypoxia group (modeling group with simulated Hypoxia environment), and Hypoxia+CVB-D group (modeling group with drug administration). The cells in the administration group were pretreated with 0.5mM CVB-D for 1 h and placed in a 37°C incubator containing 1%O2 and 5% CO2 for 6 h.

(2) Culture of H9C2 rat cardiomyocytes: Similar to primary cardiomyocytes, H9C2 cells were randomly divided into Control group, Hypoxia group, and Hypoxia+CVB-D group. Cells in the administration group were also pretreated with 0.5 mM CVB-D 1 hour before anoxic treatment, and then cultured in the same anoxic environment for 6 hours to simulate the anoxic stress response under drug intervention.

### *2.3 2,3,5-Triphenyltetrazolium Chloride (TTC) Staining*

On the first day after the construction of the mouse MI model, TTC (triphenyltetrazolium chloride) staining was used to quantify the extent of the infarct area. The mice were anesthetized and killed, and the heart tissue was quickly removed. The heart was quickly fixed by OCT at -20℃. The fixed heart tissue was sliced by a mold, and the sections were immersed in TTC staining solution with 2% concentration. After staining, the slices were photographed and recorded. Software was used to analyze the photos and measure the infarct area and non-infarct area.

### *2.4 Cardiac ultrasound detection*

One week after the establishment of the mouse model of myocardial infarction, cardiac function was assessed by cardiac ultrasound. The heart rate is controlled at 450-500 beats/min by isoflurane anesthesia and by adjusting the concentration of inhaled isoflurane. The long axis and short axis images of the heart were collected by ultrasonic probe, 5 cardiac cycles were recorded, and B-Mode and M-Mode images were obtained. Left ventricular end-systolic diameter (LVIDs), left ventricular end-diastolic diameter (LVIDd) and left ventricular ejection fraction (LVEF) were measured by software.

ISSN 2618-1584 Vol. 6, Issue 12: 72-82, DOI: 10.25236/FMSR.2024.061211

### *2.5 Masson dyeing*

One week after the establishment of a mouse MI model, we quantitatively assessed the infarct area and collagen deposition using Masson staining. During the experiment, the mice were killed after anesthesia and their hearts were quickly removed, followed by a fixed treatment with 4% paraformaldehyde and gradient dehydration with sucrose solution. After that, the dehydrated heart tissue was implanted with OCT embedding agent. The frozen section of myocardium with 10 micron thickness was obtained by freezing microtome. The sections were stained using Solebault's modified Masson tri-colour dyeing kit. After staining, the sections were sealed and recorded using a high-resolution imaging system for accurate quantitative analysis.

### *2.6 CCK-8 detection*

CCK-8 kit provided by Biyuntian (Jiangsu, China) was used to detect cell viability in strict accordance with the instructions. To assess drug toxicity and determine the optimal concentration, cells were inoculated into 96-well plates and treated with a series of concentrations of CVB-D (0mM, 0.1mM, 0.2mM, 0.5mM, 0.8mM, 1.0mM) for 24 hours when the cell fusion reached 50%. Subsequently, 10μL CCK-8 solution was added to each well, and after incubation at 37°C for 2 hours, the absorbance was measured at 450nm wavelength by enzyme-labeler. In order to explore the protective effect of drugs, the cells were also inoculated into 96-well plates, and when the cell fusion reached 50%, the cells were pretreated with 0.2 mM CVB-D for 1 hour, followed by hypoxia treatment for different periods (0h, 4h, 6h, 8h, 10h). After the treatment, CCK-8 solution was added again according to the instructions, incubated under the same conditions, and absorbance was measured to evaluate the protective effect of the drug on the cell hypoxic injury.

### *2.7 Western Blot*

Animal heart or cell samples were collected, and after thorough ultrasonic crushing treatment, the protein concentration was determined by BCA method and adjusted to a uniform concentration. Then, the protein samples of equal volume were added into each pore of SDS-PAGE gel, and electrophoretic separation was performed at a constant pressure of 80V. After electrophoresis, the film transfer operation was carried out at a constant current of 300mA for 1.5 hours at a low temperature. After the membrane transfer, 5% skim milk solution was used to seal for 2h. According to the expected molecular size of the target protein, the membrane region containing the target protein band is clipped. Next, the cut film was placed in a solution containing an appropriate amount of primary antibody and incubated overnight on a shaking bed at 4 ° C. After incubation, wash thoroughly with buffer solution. Subsequently, a solution containing goat anti-rabbit secondary antibodies was added and incubated at room temperature for 2 hours. Finally, the exposure solution is evenly dripped onto the film, which is then exposed in a gel imaging system.

### *2.8 DCFH-DA reactive oxygen species detection was co-stained with Hoechst 33342*

Under dark conditions, after removing the cell culture medium, the DCFH-DA stock solution was diluted at the ratio of DMEM 1:1000, added to the cells and incubated at 37℃ for 20 minutes. After that, the cells were cleaned with DMEM for 3 times to remove the unbound dyes. Hoechst 33342 was diluted in the same proportion and added, incubated for 10 minutes, and then cleaned with DMEM for 3 times, the cells could be observed under fluorescence microscope.

### *2.9 Ad-mCherry-GFP-LC3B dual fluorescence indicator system*

According to the current cell density, Ad-mCherry-GFP-LC3B virus was transfected at a predetermined virus titer (1×10^8 pfu/ml) and infection complex number (MOI=20) for 24 hours, and the transfected cells were subjected to subsequent specific stimulation.

### *2.10 Statistical analysis*

When comparing the two groups of measurement data, if the data is normal, t test is used; When not normal, choose non-parametric test. For the comparison of multiple sets of data, the data distribution is first evaluated by normality test before ANOVA. ANOVA is applied to normal data, and non-parametric test is applied to non-normal data. $p<0.05$ was set as the significance level, and the GraphPad Prism v8.0

ISSN 2618-1584 Vol. 6, Issue 12: 72-82, DOI: 10.25236/FMSR.2024.061211

software was used for data analysis to ensure the accuracy and visualization of results.

## 3. Results

### *3.1 CVB-D exerts a protective effect on mice after myocardial infarction in vivo*

To explore the protective effect of CVB-D on cardiac tissue in mice after myocardial infarction, TTC (triphenyltetrazolium chloride) staining, mouse echocardiographic evaluation, and Masson three-color staining were used.

On the first day after myocardial infarction, TTC staining was performed on the hearts of experimental mice to define and quantify the specific distribution and area of infarcted and non-infarcted areas. As clearly shown in Figure 1 (a-b), the heart tissue of mice in the Sham control group uniformly showed healthy red color, which reflected the good vitality of cardiomyocytes. In contrast, the hearts of mice in the myocardial infarction (MI) group showed dilated heart chambers with large white infarct areas. It is worth noting that the CVB-D treated mice showed a decreasing trend in heart infarction size compared with the MI group, suggesting that CVB-D may reduce the degree of tissue damage after myocardial infarction.

Cardiac function in mice was assessed by echocardiography on day 7 after myocardial infarction. As shown in Figure 1 (c-d), compared with the control group, the cardiac function of mice in the MI group was decreased, specifically, the myocardial contractility was significantly weakened, the ventricular wall motion amplitude was significantly decreased, the ventricular ejection fraction (LVEF) was sharply decreased from 59.3% to 28.8%, and the left ventricular short axis shortening rate (LVFS) was also decreased from 29.7% to 13.3%. After receiving CVB-D treatment, the cardiac function of mice was improved, with LVEF rising to 45.2% and LVFS rising to 22.3%, suggesting that CVB-D treatment has a positive effect on the recovery of cardiac function in mice after myocardial infarction.

In order to better understand the pathological changes of the cardiac tissue structure, we also performed Masson trichromatic staining analysis at 7 days after MI. As shown in Figure 1 (e), compared with mice in the Sham group, the hearts of mice in the MI group showed dilation of the heart cavity and thinning of the inner wall of the heart, accompanied by deposition of collagen fibers and disordered arrangement of myocardial fibers, all of which are signs of cardiac fibrosis. The mice in the CVB-D treatment group showed thickening of the inner wall of the heart and decreased deposition of collagen fibers, suggesting that CVB-D can reduce the degree of cardiac fibrosis after myocardial infarction, and may promote the repair and remodeling of cardiac tissue.

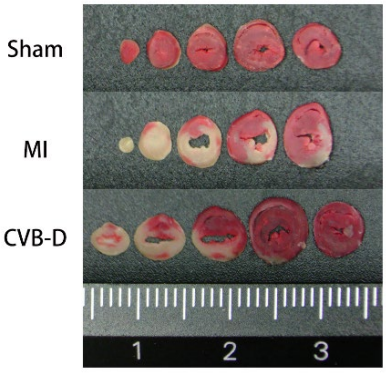


*(a) TTC staining showed the infarct area of mice in each group.*

ISSN 2618-1584 Vol. 6, Issue 12: 72-82, DOI: 10.25236/FMSR.2024.061211

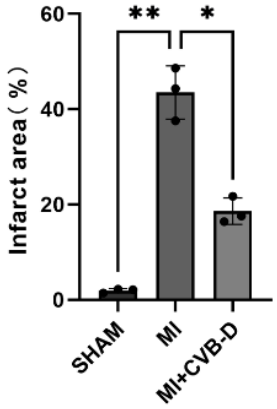


*(b) Statistical analysis of cardiac TTC staining in each group (n=3). Data are expressed as mean ± standard deviation. *p < 0.05, **p < 0.01.*

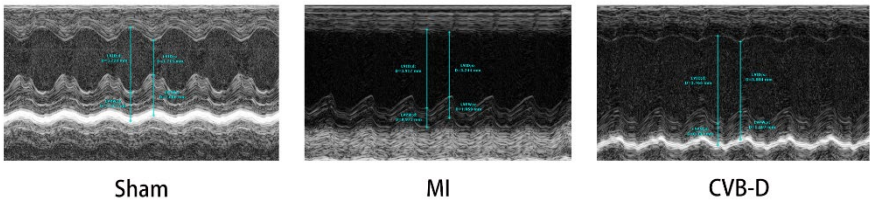


*(c) Left ventricular short-axis viscera color ultrasound images of mice in each group after myocardial infarction showed the thickness of the ventricular wall and the size of the heart cavity.*

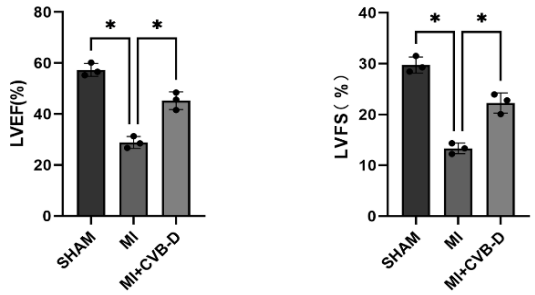


*(d) Comparison of left ventricular ejection fraction (LVEF) and left ventricular short axis shortening rate (LVFS) among all groups (n=3). Data are expressed as mean ± standard deviation. *p < 0.05*

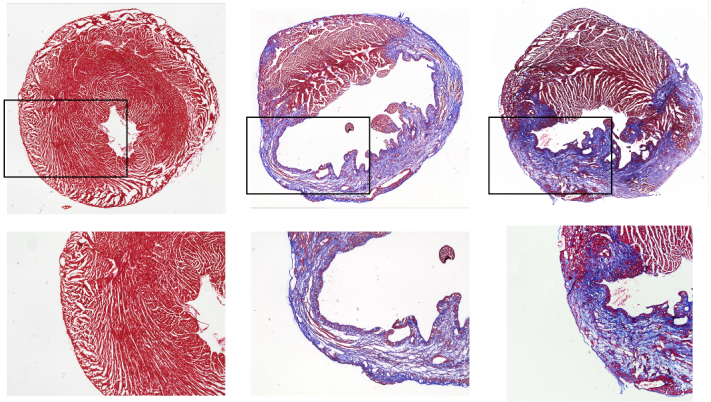

*(e) Schematic diagram of the effects of mouse myocardial infarction and CVB-D treatment on cardiac fibrosis*

*Figure 1: Effects of CVB-D on cardiac morphology and function in mice with myocardial infarction*

### *3.2 CVB-D plays a protective role on hypoxic-stimulated cells in vitro*

In order to evaluate whether CVB-D has a protective effect on hypoxic-stressed cells in vitro, this study first conducted a preliminary screening of CVB-D for H9C2 cytotoxicity using CCK-8 method,

ISSN 2618-1584 Vol. 6, Issue 12: 72-82, DOI: 10.25236/FMSR.2024.061211

aiming to determine the safe and effective dosage range of CVB-D. According to the recommendations of the existing literature, we set the concentration gradient from 0 mM to 5 mM, and introduced hypoxia stimulation as the experimental condition. The experimental results were shown in Figure 2 (a). When the concentration of CVB-D was lower than 1.0mM, the viability and survival rate of H9C2 cells showed a trend of gradual enhancement, indicating that CVB-D in this concentration range had a positive biological effect on cells. However, when concentrations increased to 1.5 mM and above, cell viability began to decline, suggesting that high concentrations of CVB-D may have toxic effects on cells. Therefore, 1.0 mM was selected as the optimal dosing concentration for subsequent experiments.

Subsequently, in order to explore the optimal time window for the protective effect of CVB-D on cells under hypoxia conditions, we applied hypoxia treatment to cells for different duration on the basis of fixed 1.0 mM concentration of CVB-D. As shown in Figure 2 (b), the cell viability of the simple hypoxia group gradually decreased with the extension of hypoxia time. The cell viability of the CVB-D group also decreased after 2 hours of hypoxia, but then the cell viability of the CVB-D group gradually increased within 2 to 6 hours and reached the maximum at 6 hours. When the period of hypoxia was extended to 8 hours or more, the cell viability showed a downward trend again. Based on the above observations, we determined that 6 hours is the time point for CVB-D to exert the best protective effect on hypoxic cells in vitro.

To further verify the protective effect of CVB-D on hypoxic-stressed cells, we used ROS staining techniques to assess changes in intracellular oxidative stress levels. Experimental results as shown in Figure 2 (c) showed that in the Control group, cells showed a weak green fluorescence signal, while in the hypoxic treatment group, the green fluorescence signal was significantly enhanced, with statistical significance, which may be due to the intensification of oxidative stress in cells induced by hypoxia. In contrast, the cells treated with CVB-D showed a significantly reduced green fluorescence signal, suggesting that CVB-D can alleviate the oxidative stress response caused by hypoxia.

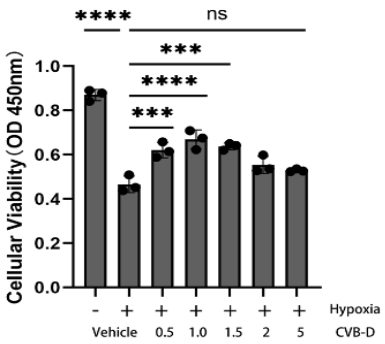


*(a) Effects of different concentrations of CVB-D on H9C2 cell viability. The cells were treated with different concentrations of CVB-D and hypoxia for 6 h. The cell viability was evaluated by CCK-8 assay. Data are expressed as mean ± standard deviation, n=3. ***p < 0.001, ****p <0.0001.*

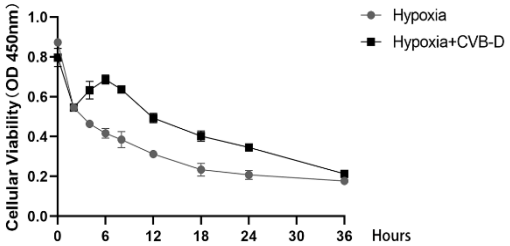


*(b) Evaluation of the protective effect of CVB-D on hypoxic H9C2 cells at different time points. After the cells were pretreated with 1.0 mM CVB-D for 1 hour or without drug intervention, they were subjected to hypoxia treatment at different times (0h, 2h, 4h, 6h, 8h, 12h, 18h, 24h, 36h), and then the cell viability was evaluated by CCK-8 assay.*

ISSN 2618-1584 Vol. 6, Issue 12: 72-82, DOI: 10.25236/FMSR.2024.061211

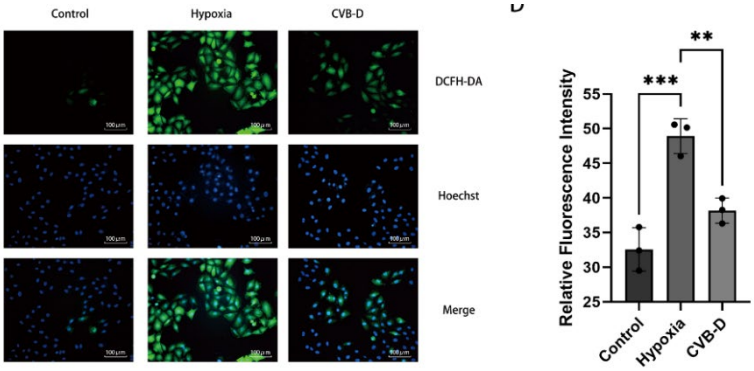


*(c) Effect of CVB-D on oxidative stress response of cardiomyocytes induced by hypoxia. After the cells were pretreated with 1.0 mM CVB-D, they were subjected to 6-hour hypoxia treatment, and the intracellular ROS levels were evaluated by DCFH-DA staining. Hoechst 33342 is used for nuclear staining. Data are expressed as mean ± standard deviation, n=3. **p < 0.01, ***p < 0.001.*

*Figure 2: Assessment of protective effects of CVB-D on H9C2 cardiomyocytes under hypoxia*

### *3.3 Protective mechanism of CVB-D on mice with myocardial infarction and hypoxia-induced cell model: enhancing autophagy and promoting smooth autophagy flow*

In order to further explore the specific action path of CVB-D in mice with myocardial infarction and in vitro hypoxia-induced cell models, this study focused on autophagy, a cellular biological process, in view of its protective effect in the early stage of the disease. In this study, an anoxic model of H9C2 cells was constructed in vitro to detect the protein expression ratio of autophagy marker LC3II/LC3I. Results As shown in Figure 3 (A), the ratio of LC3II/LC3I in cells of the hypoxic group was significantly higher than that of the control group. After CVB-D treatment, the expression ratio of this autophagy marker was further increased compared with that of hypoxia group, suggesting that CVB-D enhanced the early autophagy process.

In addition, this study also verified the effect of CVB-D on autophagy flow. Lamp1 (lysosomal associated membrane protein 1) is a lysosomal membrane protein, and its change is usually related to the function and number of lysosomes. When its expression is decreased, it may indicate that the lysosomal function is impaired or the fusion between the autophagosome and the lysosome is blocked, and the autophagy flow is poor. As a selective autophagy receptor, an increase in the level of p62 may indicate a decrease in autophagy activity or the inability of lysosomes to effectively degrade p62 and its binding substrate, and the autophagy flow is blocked [9]. As shown in Figure 3 (a), after hypoxia treatment for 6 hours, LC3II/LC3I protein expression ratio was observed to increase, while Lamp1 expression decreased and p62 expression increased. These changes indicated that autophagy flow was blocked under hypoxia conditions, resulting in the inability of autophagosomes to effectively fusion with lysosomes for degradation, thus worsening cell damage. However, when the cells received CVB-D intervention, the expression ratio of LC3II/LC3I protein increased, while the expression of Lamp1 increased, and the expression of p62 decreased. These changes indicate that CVB-D can restore and promote the smooth progress of autophagy flow, thus alleviating the cell damage caused by hypoxia.

In order to further explore the regulation of CVB-D on autophagy flow of cardiomyocytes, Yuan dynasty cardiomyocytes were isolated and cultured from heart tissues of 1-day-old mice after birth. mcherry-GFP-LC3 tandem fluorescently labeled adeno-associated virus was introduced in advance for cell transfection to achieve visual tracking of autophagy process: When red fluorescence overlaps with green fluorescence to form yellow particles, it indicates a large amount of autophagy accumulation, that is, the autophagy flow is blocked and the degradation process is not smooth; On the contrary, if only red fluorescent particles are observed, and the green fluorescence is significantly reduced or even disappeared, it indicates that the autophagosome has effectively fused to the autophagolysosome and has been degraded, indicating the smooth progress of autophagy flow. The fluorescence results of this study showed in Figure 3 (b) that no obvious autophagy related fluorescence particles were found in the cardiomyocytes of the Control group, while under simulated hypoxia conditions, a large number of yellow fluorescent particles were rapidly accumulated in the cardiomyocytes, reflecting the accumulation of autophagosomes induced by hypoxia stress, that is, the inhibition of autophagy flow. It is worth noting that after the intervention of CVB-D, the number of green fluorescent particles in the cell decreased, and the number of red fluorescent particles was mainly reduced, and the number of red fluorescent particles

ISSN 2618-1584 Vol. 6, Issue 12: 72-82, DOI: 10.25236/FMSR.2024.061211

was less than that in the hypoxia group, suggesting that CVB-D may promote the fusion of autophagosome and lysosome and the degradation of contents through some mechanism, thus effectively improving the autophagy flow block state caused by hypoxia.

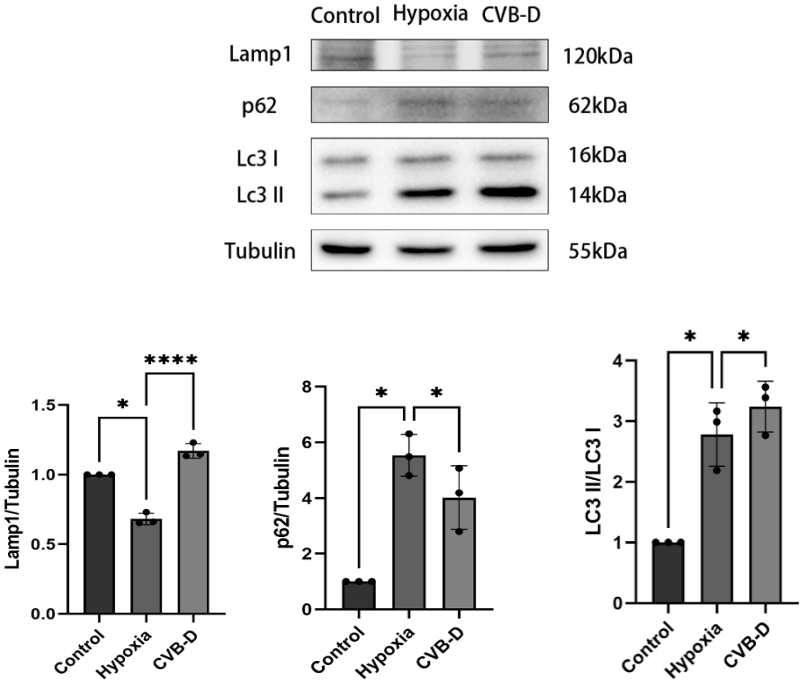


*(a) The effect of CVB-D on the expression of autophagy markers in cardiomyocytes. LC3II/LC3I ratio, Lamp1 and p62 protein expression were detected by Western Blot. Data are expressed as mean ± standard deviation, n=3. *p < 0.05, ****p < 0.0001.*

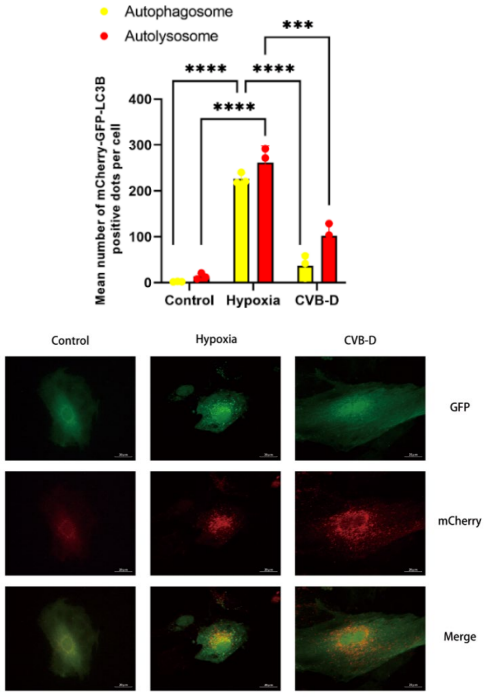


*(b) Expression of Ad-mCherry-GFP-LC3B dual fluorescence indicator system in cardiomyocytes. After transfection with Ad-mCherry-GFP-LC3B virus, primary cardiomyocytes were pretreated with 1.0 mM CVB-D and then treated with hypoxia. The fusion of autophagosome and lysosome was observed by fluorescence microscopy. The yellow arrow indicates the autophagosome formed by the fusion of the autophagosome and the lysosome. The scale is 20μm*

*Figure 3: CVB-D promotes the patency of autophagy flow in cardiomyocytes*

ISSN 2618-1584 Vol. 6, Issue 12: 72-82, DOI: 10.25236/FMSR.2024.061211

### *3.4 CVB-D may alleviate hypoxic-induced injury via Ets1/Mcl-1 pathway*

In view of the fact that Ets1, as a key transcription factor, shows its unique regulatory potential when cells respond to environmental stress, especially after its nuclear translocation activation, it can accurately bind to the promoter sequence of specific genes, and then regulate the transcriptional activity of downstream genes, profoundly affecting the physiological state and fate choice of cells [10-13]. Previous studies have shown that Ets1 promotes autophagy through its nuclear translocation mechanism, and Mcl-1, as a potential downstream effector molecule in this process, is also finely regulated by Ets1 [14]. Based on this, this study explored in depth whether CVB-D might play a positive role in protecting cells from hypoxia damage by mediating the Ets1/Mcl-1 signaling pathway.

To verify the above hypothesis, we quantitatively analyzed the protein expression levels of Ets1 and Mcl-1 in the mouse model and H9C2 myocardial cell line by Western Blot. Figure 4 (a) shows that compared with the normal control group, the expressions of Ets1 and Mcl-1 in the myocardial infarction (MI) model group showed A significantly up-regulated trend, suggesting that the two may play an important role in the response of cells to hypoxia stress. Notably, the expression levels of Ets1 and Mcl-1 were further increased when CVB-D was given, both in vivo and in H9C2 cells, which supports the possibility that CVB-D may enhance the resistance of cells to hypoxic damage by activating the Ets1/Mcl-1 pathway.

To further elucidate the central role of Ets1 in CVB-D-mediated protective effects, we introduced Ets1 specific inhibitor TK216 into H9C2 cell system. As shown in Figure 4 (b), the addition of TK216 effectively inhibited the activity of Ets1, and subsequently led to a significant downregulation of the expression level of Mcl-1. This finding suggests that Ets1 plays an upstream role in regulating the expression of Mcl-1, and reveals that CVB-D protects cells from hypoxic damage through Ets1/Mcl-1 pathway.

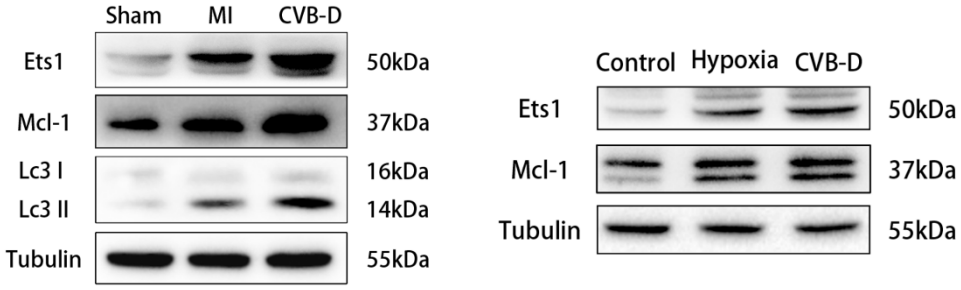


*(a) Through Ets1/Mcl-1 pathway. Effects of CVB-D on the expression of Ets1 and Mcl-1 proteins in myocardial infarction mice and H9C2 cardiomyocytes. The expression levels of Ets1 and Mcl-1 were detected by Western Blot.*

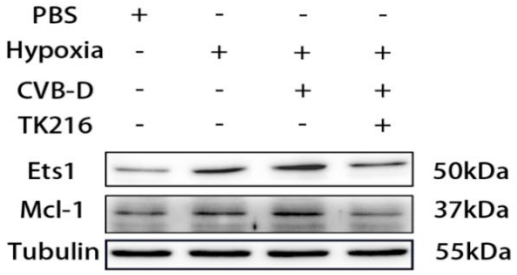


*(b) The effect of Ets1 specific inhibitor TK216 on Mcl-1 expression. After H9C2 cardiomyocytes were treated with TK216 for 24h, the expression levels of Ets1 and Mcl-1 protein were detected by Western Blot.*

*Figure 4: CVB-D alleviates hypoxia-induced cardiomyocyte injury*

## 4. Discuss

This study investigated the protective effect of Cyclovirobuxine D (CVB-D) in Myocardial Infarction (MI) and its potential molecular mechanism in vivo and in vitro.

ISSN 2618-1584 Vol. 6, Issue 12: 72-82, DOI: 10.25236/FMSR.2024.061211

We evaluated cardiac function in mice with myocardial infarction after CVB-D treatment using ultrasound imaging technique. The results showed that CVB-D treatment improved the cardiac function of mice after myocardial infarction. TTC staining and Masson trichromatic staining further confirmed that CVB-D reduced the infarct size and the degree of cardiac fibrosis after myocardial infarction. These results suggest that CVB-D can improve cardiac structure and function after myocardial infarction in vivo.

In this study, we used CCK8 cell activity detection and ROS level assessment to verify the ability of CVB-D to effectively alleviate hypoxic-induced myocardial cell damage in vitro in the H9C2 cardiomyocyte model. At the same time, through CCK8 analysis, we determined that CVB-D showed protective effects in the early stages of hypoxic injury, which prompted us to focus our research on the process of autophagy.

Autophagy, as a key intracellular self-degradation and recycling mechanism, has been widely recognized as an important regulatory factor for myocardial cell survival after myocardial infarction [8]. In this study, we observed that CVB-D treatment enhanced the autophagy activity of cardiomyocytes and promoted the patency of autophagy flow. At the protein level, this effect is manifested by an increase in the ratio of LC3-II/I, the signature protein of autophagy, accompanied by a decrease in the expression of p62 protein and an up-regulation of the lysosomal associated membrane protein Lamp1. We used Ad-mCherry-GFP-LC3B dual fluorescence reporting system to verify the ability of CVB-D to promote the fusion of autophagosomes and lysosomes and the effective degradation of their contents, thus clarifying the role of CVB-D in improving the hypoxia-induced autophagy flow retardation.

As a transcription factor, Ets1 plays a key role in a variety of cellular processes [15]. Our study is the first to reveal the protective effect of CVB-D on cardiomyocytes via the Ets1/Mcl-1 signaling pathway. By Western Blot, we found that CVB-D could increase the expression levels of Ets1 and Mcl-1. In addition, experiments using Ets1 specific inhibitor TK216 further confirmed the upstream regulatory role of Ets1 in CVB-D-mediated myocardial protection. These results suggest that CVB-D may promote the expression of Mcl-1 by activating Ets1, and participate in the autophagy process of cardiomyocytes.

Although this study provides preliminary evidence for the potential protective effects and molecular mechanisms of CVB-D in myocardial infarction, there are still some limitations. First of all, this study focused on the effect of CVB-D on autophagy of cardiomyocytes, while the long-term effects of CVB-D in myocardial infarction still need to be further studied. Second, this study failed to fully elucidate the detailed molecular mechanism of Ets1/Mcl-1 signaling pathway in CVB-D-mediated myocardial protection, and future studies will further explore the upstream and downstream regulatory network of this pathway.

This study not only provides new strategies and potential drug targets for the treatment of myocardial infarction, but also provides insights for further understanding the mechanism of autophagy regulation of cardiomyocytes under stress conditions. Future studies will continue to explore the potential application of CVB-D in the treatment of cardiovascular disease and further elucidate its molecular mechanism of action.

## References

*[1] Hu, C., X. Zhang, T. Teng, et al. Cellular Senescence in Cardiovascular Diseases: A Systematic Review. Aging and Disease, 2022. 13(1): p. 103-128.*

*[2] Song, P., Q. Zhao, and M.-H. Zou, Targeting senescent cells to attenuate cardiovascular disease progression. Ageing Research Reviews, 2020. 60: p. 101072.*

*[3] Gao G, Fu L, Xu Y, et al. Cyclovirobuxine D Ameliorates Experimental Diabetic Cardiomyopathy by Inhibiting Cardiomyocyte Pyroptosis via NLRP3 in vivo and in vitro. Front Pharmacol. 2022 Jul 5;13: 906548.*

*[4] Hu D, Liu X, Wang Y, et al. Cyclovirobuxine D ameliorates acute myocardial ischemia by K(ATP) channel opening, nitric oxide release and anti-thrombosis. Eur J Pharmacol. 2007 Aug 13;569(1-2):103-9.*

*[5] Yu B, Fang TH, Lü GH, et al. Beneficial effect of Cyclovirobuxine D on heart failure rats following myocardial infarction. Fitoterapia. 2011 Sep;82(6):868-77.*

*[6] Wang S, Xia P, Rehm M, et al. Autophagy and cell reprogramming. Cell Mol Life Sci. 2015 May; 72(9):1699-713.*

*[7] Gu S, Tan J, Li Q, et al. Downregulation of LAPTM4B Contributes to the Impairment of the Autophagic Flux via Unopposed Activation of mTORC1 Signaling During Myocardial Ischemia/*

ISSN 2618-1584 Vol. 6, Issue 12: 72-82, DOI: 10.25236/FMSR.2024.061211

*Reperfusion Injury. Circ Res. 2020 Sep 11;127(7):e148-e165.*
*[8] Zhang X, Wang Q, Wang X, et al. Tanshinone IIA protects against heart failure post-myocardial infarction via AMPKs/mTOR-dependent autophagy pathway. Biomed Pharmacother. 2019 Apr;112: 108599.*
*[9] Lv Xiaoxi, Hu Zhuowei. Detection of autophagy flow. Acta Pharmacologica Sinica, 2016,51(1): 45-51. (in Chinese)*
*[10] Wang T, Ba X, Zhang X, et al. Nuclear import of PTPN18 inhibits breast cancer metastasis mediated by MVP and importin β2. Cell Death Dis. 2022 Aug 18;13(8):720.*
*[11] Peng Y, Li H, Wu M, et al. NGX6 inhibits AP-1 and Ets-1 expression and down-regulates cyclin D1 in human colorectal cancer. Acta Biochim Biophys Sin (Shanghai). 2009 Jun;41(6):504-14.*
*[12] Zadora PK, Chumduri C, Imami K, et al. Integrated Phosphoproteome and Transcriptome Analysis Reveals Chlamydia-Induced Epithelial-to-Mesenchymal Transition in Host Cells. Cell Rep. 2019 Jan 29; 26(5):1286-1302.e8.*
*[13] Huang J, Chen Z, Ye Y, et al. DTX3L Enhances Type I Interferon Antiviral Response by Promoting the Ubiquitination and Phosphorylation of TBK1. J Virol. 2023 Jun 29;97(6):e0068723.*
*[14] Selimovic D, Porzig BB, El-Khattouti A, et al. Bortezomib/proteasome inhibitor triggers both apoptosis and autophagy-dependent pathways in melanoma cells. Cell Signal. 2013 Jan;25(1):308-18.*
*[15] Zhang W, Zhao J, Lee JF, et al. ETS-1-mediated transcriptional up-regulation of CD44 is required for sphingosine-1-phosphate receptor subtype 3-stimulated chemotaxis. J Biol Chem. 2013 Nov 8; 288(45):32126-32137.*